

Disturbance mechanism of coal mining subsidence to typical plants in a semiarid area using O–J–I–P chlorophyll *a* fluorescence analysis

Y. LIU*, S.G. LEI**,+, X.Y. CHEN*, M. CHEN*, X.Y. ZHANG*, and L.L. LONG*

*The State Key Laboratory of Mining Response and Disaster Prevention and Control in Deep Coal Mine, School of Earth and Environment, Anhui University of Science and Technology, Huainan, 232001, China**

*Engineering Research Center of Ministry of Education for Mine Ecological Restoration, China University of Mining and Technology, Xuzhou, 221116, China***

Abstract

The response of individual plants to coal mining subsidence disturbance reflects the micro-ecological mechanism implied in the macro-response, which is the basis of studying the rule of vegetation disturbance of large-scale coal mining. In this study, O–J–I–P chlorophyll *a* fluorescence analysis was used to diagnose the disturbance mechanism of typical individual plants by coal mining subsidence in a semiarid area. The results showed that the groundwater level and soil water content decreased due to the disturbance of coal mining subsidence and the plant growth was affected by drought stress. The rapid chlorophyll fluorescence induction curve of leaves was deformed, the stomatal limitation increased, and the photosynthetic electron transfer was inhibited. Stomatal conductance, photosynthetic rate, and transpiration rate decreased significantly. The spatial heterogeneity of soil water content after mining subsidence is the main reason for the differing degree of plant drought stress in different subsidence areas.

Keywords: chlorophyll *a* fluorescence; drought stress; mine environment; photosynthetic activity; soil disturbance.

Introduction

Coal, which serves as the primary energy source in China, contributes to more than 60% of the disposable energy production and consumption and will comprise approximately 90% of China's fossil energy resources by the end of 2020 (Wang *et al.* 2018a). The status of coal as the main source of energy will not change for a long time (Yuan *et al.* 2018). The major coal bases in China are primarily distributed in the western regions (Liu and Li 2019). However, the water resources of the semiarid areas in Western China only comprise 8.3% of the total water resources in China owing to the geographical location and climate, which leads to a lack of water resources and an extremely fragile ecological environment (Liu

et al. 2019a). With the shift in the focus of coal mining to the western region, high-intensity and large-scale underground coal mining inevitably cause the degradation of land quality, reduction of vegetation coverage, and intensification of surface deserts (Chiochetta *et al.* 2017, Karan and Samadder 2018, Yang *et al.* 2018a), which adds considerable pressure to the local eco-environment, and forms the contradiction between the environmental damage of coal mining and the sustainable utilization of mine land. Statistics indicate that the subsidence area of coal mining land in China is still increasing at the rate of 2.7–4.1 million ha per year, and with the continuous development of the coal industry and the gradual increase in coal production, the area of subsidence is increasing further (Sun *et al.* 2019). Surface subsidence, caused by

Received 25 July 2020, accepted 5 October 2020, published online 23 October 2020.

*Corresponding author; e-mail: lsgang@126.com

Abbreviations: ABS/RC – absorption flux per RC; AN – ammonium nitrogen; BD – soil bulk density; CK – control area; CZ – compression zone; DF_(abs) – driving force of photosynthesis; DI₀/RC – energy dissipation per RC; E – transpiration rate; ET₀/ABS – quantum yield for electron transport (*t* = 0); ET₀/RC – trapping energy used for electron transport per RC; ET₀/TR₀ – probability that a trapped exciton moves an electron into the electron transport chain beyond Q_A[–] (*t* = 0); F₀ – minimal fluorescence, when all PSII RCs are open; F₀/F_m – thermal dissipation quantum yield; F_m – maximal fluorescence at P-step, when PSII RCs are closed; F_v – maximum variable fluorescence; F_v/F_m – maximal photochemical efficiency of PSII; g_s – stomatal conductance; L_s – stomatal limitation; M₀ – approximated initial slope of the fluorescent transient; NDVI – normalized difference vegetation index; NN – nitrate nitrogen; NZ – neutral zone; OM – soil organic matter; PI_{ABS} – performance index based on absorbed light energy; P_N – photosynthetic CO₂ assimilation rate; SWC – soil water content; SZ – stretch zone; TN – total nitrogen; TP – total phosphorus; TR₀/ABS – maximum quantum yield for primary photochemistry (*t* = 0); TR₀/RC – trapping flux leading to Q_A reduction per RC; V_J – relative variable fluorescence at J-step (2 ms); V_K – relative variable fluorescence at 300 μs (K-band).

Acknowledgments: This work was supported by the National Key Basic Research and Development Program (2013cb227904) and the National Natural Science Foundation of China (13612059). We thank the anonymous reviewers for improving the quality of the manuscript.

Conflict of interest: The authors declare that they have no conflict of interest.

large-scale underground coal mining, affects the topography, hydrology, soil physico-chemical properties, and other factors of plant habitats (Lechner *et al.* 2016, Yang *et al.* 2018a). Mining activity is one of the most important causes of the disturbance of land and vegetation in mining areas. Therefore, studying the disturbance mechanism of mining activities to plant growth in semiarid areas is strongly merited, and such studies can provide a basis for the sustainable management of the mining environment and the restoration of production capacity of mining land in Western China.

The impact of underground mining activities on the eco-environment, particularly on vegetation in semiarid areas, such as the Loess Plateau, is a particular concern (Darmody *et al.* 2014, Lechner *et al.* 2016, Yang *et al.* 2018a, Hu *et al.* 2020). One feature of the highly destructive anthropogenic activity of underground coal mining is that it often seriously disturbs the site surface conditions for plant growth (Wang and Zhao 2017, Jia 2018, Liu *et al.* 2019b). Underground mining usually raises public concern because this type of disturbance may insidiously and catastrophically result in consequences, such as the degradation of vegetation succession and the deterioration of ecosystems (Eckert *et al.* 2015, Lei *et al.* 2016, Yang *et al.* 2018a). Studies of the consequences of the disturbance of vegetation owing to underground mining began around 2000 in the semiarid area of the Loess Plateau (Yang *et al.* 2018b). Most of the relevant literature has involved monitoring and assessing the subsidence of land, degradation of land quality, and negative impacts on vegetation. Recent achievements in this field include the use of remote sensing and mathematical model-based methods to assess coal mining subsidence (Zhang *et al.* 2015, Rošer *et al.* 2018), the changes of soil physicochemical properties (Yang *et al.* 2016, Wang *et al.* 2017, Ma *et al.* 2019), as well as the mitigation of subsidence influences (Luo 2008, Lv 2016) and the restoration of the disturbed land that resulted from mining (Clifford *et al.* 2019, Feng *et al.* 2019, Wang *et al.* 2020). Some studies have focused on the broader changes of vegetation in the Loess Plateau coal mining area, where different scale observations derived from satellite imagery have determined that the vegetation coverage and biomass index is dynamic, and coal mining is one of the factors that drives the change in vegetation (Lei *et al.* 2016, Li *et al.* 2019, Liu *et al.* 2019a,c). On a local scale, namely, the area of an above underground mining operation, the mechanism of influence of underground mining on individual vegetation is not well understood. This limited the development of practical strategies and approaches used to achieve the goals of environmental protection and sustainable or green mining (Darmody *et al.* 2014). In this regard, more research is needed to reveal and sustainably manage the vegetation at underground mining areas (Liu *et al.* 2019a).

Vegetation, the main body of terrestrial ecosystems, is the link between the atmosphere, soil, water, and other natural elements (Vereecken *et al.* 2016). Exploration of the disturbance mechanism of coal mining subsidence on typical plants in semiarid areas is the key to the

sustainable development of the ecological environment of mines, a judgment of the benign succession of mine ecology, and guidance of the restoration of environments damaged by mining (Bian *et al.* 2018, Yang *et al.* 2018b). The response of individual plants to the disturbance from coal mining subsidence reflects the micro-ecological mechanism implied in the macro-response, which is the basis of studying the disturbance law of vegetation caused by large-scale underground coal mining (Yu *et al.* 1997). But how does coal mining subsidence affect the individual growth of surface plants? What are the key soil environmental factors that affect the growth of vegetation in subsidence areas? The damage to individual plants in a subsidence area is closely related to the disturbance of the root environment by collapse, which shows that the growth of the plant is subjected to the stress of environmental disturbance (Liu *et al.* 2019a). As a classical monitoring method of photosynthesis, chlorophyll (Chl) fluorescence induction technology has become one of the most powerful and widely used technologies in the field of plant ecological research (Gray *et al.* 2006, Carstensen *et al.* 2019). It is known as an effective probe for the state of plant stress and can quickly obtain the information on photochemical activity and electron transfer of PSII and analyze the kinetic curve of Chl fluorescence induction (JIP-test). Thus, it has become a powerful tool to study the effects of stress on plant photosynthesis (Mehta *et al.* 2010). Dąbrowski *et al.* (2016) used Chl *a* fluorescence to quickly diagnose the changes of PSII structure in ryegrass under salt stress. Zushi and Matsuzoe (2017) used Chl *a* fluorescence O–J–I–P transients to analyze salt stress in the leaves and fruits of tomato (*Solanum lycopersicum*).

In summary, understanding how underground mining results in disturbance and stress on surface plants is a current scientific and practical issue that strongly merits further study, particularly in arid and semiarid areas such as the Loess Plateau. However, at the individual scale, empirical studies on the response and sustainability of surface plants in underground mining areas are still lacking. The process of underground mining and the factors that cause the disturbance of plant growth are not well understood. This paper examined a semiarid mining area that is experiencing underground mining. The goals of this paper were: (1) to diagnose the disturbance of plants in the subsidence area using O–J–I–P Chl *a* fluorescence analysis, (2) to screen the physicochemical properties of the main soil that affect the individual growth of plants in the subsidence area, and (3) to reveal the transfer process of mining subsidence disturbance to individual plants, provide insights into sustainable management and guide the restoration for vegetation in the mining area.

Materials and methods

Study area: This study was conducted at the 52302 coal mining working face of the Daliuta Coal Mine at the northern edge of the Loess Plateau, Shenmu City, Shaanxi Province, Western China (110°12'23" to 110°22'54"E and 39°13'53" to 39°22'32"N, Fig. 1). The study area, dominated

by annual grasslands, deciduous broad-leaved shrubs, and other desert plants, covers a total area of more than 376 km². This environment is characterized by a typical arid and semiarid continental climate of a plateau with a dry climate and low rainfall. The average annual rainfall and evaporation are 413.5 mm and 2,111.2 mm, respectively. The main soil types are loess and aeolian sandy soil that have a loose structure, poor resistance to erosion, and vulnerability to wind erosion. Human production activities in the mining area have led to the destruction and replacement of the original vegetation with artificial restoration species (Liu *et al.* 2019a). The area was first mined 10 years ago and is currently being subjected to a second mining operation. The working face, with a coal seam depth, which is approximately 220 m long and 7 m wide with a speed of advancement of 12 m per day, belongs to a typical high-intensity and extremely large working face mining area. Under these conditions, the surface of the earth is sinking violently, and the deformation is concentrated. The subsidence cracks or sinking basins form rapidly on the ground surface. Mining subsidence theory (He 1991) indicates that the subsidence basin is divided into a stretch zone (SZ), compression zone (CZ), and neutral zone (NZ). The area, which is not disturbed by coal mining and has the same topography and landform, was established as the control area (CK).

Selection of typical plants: *Artemisia ordosica* Krasch. (semi-shrub), *Caragana korshinskii* Kom. (shrub), and the dominant species *Populus* spp. (arbor) were selected as typical plant species to monitor in this area. The vegetation at the 52302 working face consists primarily of deciduous bushes, hay prototypes, and desert species, with *A. ordosica*, *C. korshinskii*, and *Populus* spp. as the main representatives of the vegetative growth of psammophytes

in semi-fixed sand, fixed sand, and sand dune lowlands. *Populus* spp. has an obvious quantitative advantage among trees in the mining subsidence areas because their population is denser than those of other plants.

Chl fluorescence and JIP-test parameters: To eliminate the influence of plant age, leaf position, temperature, light intensity, air humidity, measurement time, and other factors on Chl fluorescence, three plants (*A. ordosica*, *C. korshinskii*, and *Populus* spp.) with the same growth status, terrain, and elevation and complete root system were selected as the research objects. The plant leaves without overlapping each other were selected for determination. The Chl fluorescence and JIP parameters of the first three mature leaves in the vertically downward direction of the main stem were measured, and each selected leaf was measured three times. Three replicates of each plant were determined in four plots (SZ, CZ, NZ, and CK).

Field measurement of Chl *a* fluorescence was carried out from 13 August 2018 to 25 August 2018, when the cracks in ground subsidence were forming in the study area. Chl fluorescence measurements were performed using a *Handy PEA* continuous excitation plant efficiency analyzer (*Hansatech Instruments, Ltd.*, Norfolk, UK) from 8:30 to 12:00 h. The light source was red light with a wavelength of 650 nm, and the intensity of illumination was 3,500 $\mu\text{mol}(\text{photon}) \text{ m}^{-2} \text{ s}^{-1}$. The fluorescence signal was recorded with a maximum frequency of 10^5 points s^{-1} (each 10 μs) within 0–0.3 ms (Brestic *et al.* 2012, Liu *et al.* 2019a), after which the frequency of recording gradually decreased, resulting in the collection of 118 points within 1 s. The Chl fluorescence induction curve was measured shortly after the selected leaves were maintained in the dark for 20 min.

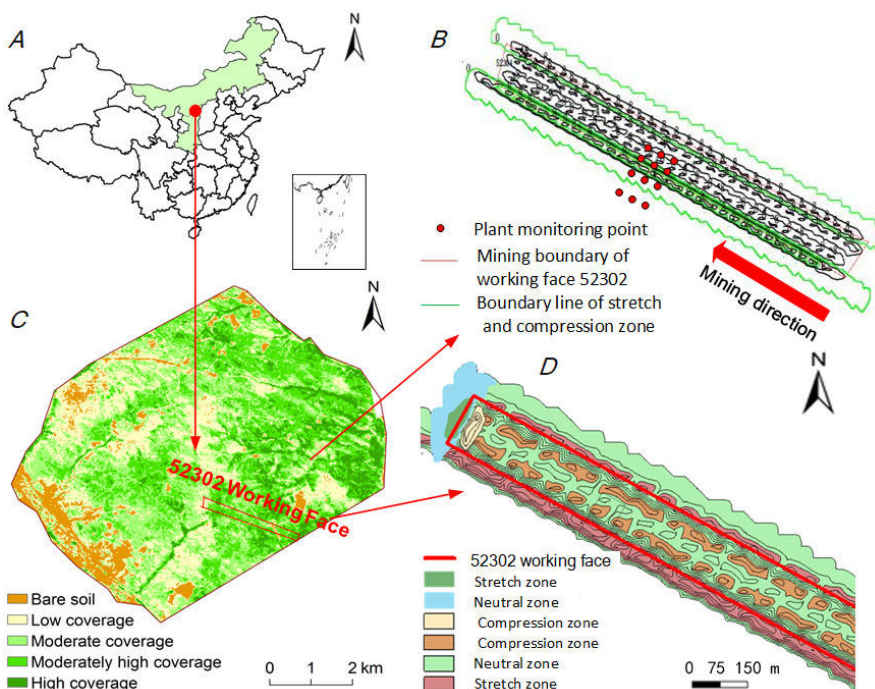


Fig. 1. The location of the study area and the plan of field plant monitoring and investigation. (A) The geographic location of Daliuta coal mine; (B) the geographic location and vegetation cover of 52302 working face; (C) field plant monitoring and investigation point; (D) division of stretch zone (SZ), compression zone (CZ), neutral zone (NZ) above working face surface.

Chl *a* fluorescence transient data were used to calculate basic parameters and the parameters required for the JIP-test. The main fluorescence parameters (F_v/F_m , F_v/F_0 , PI_{ABS} , M_0 , ABS/RC , ET_0/RC , DI_0/RC , ET_0/TR_0 , $DF_{(abs)}$, and TR_0/RC) were calculated, and the specific meanings are described in detail by Strasser *et al.* (2004), Dąbrowski *et al.* (2015), Kalaji *et al.* (2018), and Singh and Prasad (2015). The parameters of Chl *a* fluorescence transient are summarized in 'Abbreviations'. The relative variable fluorescence intensity (V_t) and the difference of relative variable fluorescence intensity (ΔV_t) were calculated as described by Su *et al.* (2013): $V_{t,i} = (F_{t,i} - F_{0,i})/(F_{m,i} - F_{0,i})$, $\Delta V_{t,i} = V_{t,i} - V_{t,CK}$, where *i* indicates fluorescence parameters in different study plots (SZ, CZ, NZ, and CK). The ΔK -band, ΔJ -band, and ΔI -band were measured for 300 μ s, 2 ms, and 30 ms, respectively, to determine the ΔV_t (Su *et al.* 2013).

Photosynthetic parameters: The field measurement of photosynthetic parameters was conducted simultaneously with the measurement of Chl fluorescence, and three replicates for each selected leaf. The photosynthetic CO_2 assimilation rate (P_N), stomatal limitation (L_s), stomatal conductance (g_s), and transpiration rate (E) of selected leaves were measured using an *LCI-SD* portable photosynthesis measurement system (*Li-Cor*, Lincoln, NE, USA) under natural solar irradiance (PPFD of 1,500–1,600 μ mol $m^{-2} s^{-1}$). The temperature of the leaf chamber was 20–25°C. The environmental CO_2 concentration was 385–400 μ mol mol^{-1} . After removing dust from the leaf surface and induction for 30 min at saturation light intensity, parametric measurements were collected on mature and fully expanded leaves.

Soil physico-chemical properties: To analyze the influence of soil physico-chemical properties on the JIP-test and photosynthetic parameters of plant leaves, it was necessary to collect synchronously the root soil of selected plants in four plots (SZ, CZ, NZ, and CK) when measuring Chl fluorescence and photosynthetic parameters. The location of sampling points was recorded using a portable global positioning system (GPS) (*eTrex Venture*, *Garmin*, Lenexa, KS, USA). Litter on the surface of the soil was removed before sampling, and then 0–30 cm of soil was collected. Three samples were collected from each sampling point, and the values of the three samples were averaged. The collected soil samples (approximately 50 g) were stored in sealed bags, marked, and taken back to the laboratory for testing. The physico-chemical properties of soil primarily include the soil water content (SWC), soil organic matter (OM), total nitrogen (TN), total phosphorus (TP), ammonium nitrogen (AN), nitrate nitrogen (NN), and soil bulk density (BD). The soil moisture was determined as described in Chen *et al.* (2017), and the soil nutrient contents were determined as described by Liu *et al.* (2019a).

Statistical analysis: Statistical analyses of the data were conducted using *Microsoft Excel 2013* (Microsoft, Inc., Redmond, WA, USA). The data analysis software

OriginPro, v. 9.0 (*OriginLab, Inc.*, Northampton, MA, USA) was used to compare the differences of the Chl fluorescence induction curve, the parameters of the JIP-test, and photosynthetic performance in four survey plots (SZ, CZ, NZ, and CK). The relationship between soil physicochemical properties and JIP-test parameters, as well as that of the photosynthetic parameters, was analyzed using *Matlab* software, v. 2017b (*The MathWorks, Inc.*, Nedick, MA, USA). The transfer process of coal mining subsidence on plant growth in semiarid areas was drawn using *Microsoft PowerPoint 2013* (*Microsoft, Inc.*). Four photosynthetic parameters (P_N , L_s , g_s , E) were executed to the study of variance (ANOVA) to determine the significant differences between four different subsidence locations using software *OriginPro*, v. 9.0.

Results and discussion

Rapid Chl fluorescence induction curve: The fluorescence response characteristics of *Populus* spp., *C. korshinskii*, and *A. ordosica* in SZ, CZ, NZ, and CK were monitored using an O–J–I–P Chl *a* fluorescence analysis. The rapid Chl fluorescence induction kinetic curve (O–J–I–P) can provide the information on PSII photochemistry, accurately and quickly reflect the redox state of the PSII donor side, acceptor side, and PSII reaction center in the light reaction. The O–J–I–P curves of *Populus* spp., *C. korshinskii*, and *A. ordosica* in the subsidence of SZ, CZ, NZ, and CK are shown in Fig. 2. The O–J–I–P curves in the leaves of three plants exhibited spatial heterogeneity in different subsidence areas of the working face. Compared with the CK, different degrees of heterogeneity were observed in the O–J–I–P curves of *Populus* spp., *C. korshinskii*, and *A. ordosica* leaves in SZ, CZ, and NZ. The degree of variation of the SZ curve was the largest, followed by CZ, and that of the O–J–I–P curve in NZ was much smaller compared with those of CZ and SZ. This indicated that coal mining subsidence caused disturbance to the O–J–I–P curves of plant leaves, and the effects of disturbance in SZ and CZ were more noticeable than those in the CK.

As shown in Fig. 2, different plant species varied in their resistance to the disturbance caused by coal mining subsidence. The rapid Chl fluorescence induction curve of different plant leaves was deformed, and the relative fluorescence value of the K–J–I segment increased differently. The change in the relative fluorescence for *A. ordosica* was the smallest, and that of *Populus* spp. was the largest. Therefore, *A. ordosica* and *C. korshinskii*, which have small leaves and deep roots, resist stress more strongly and are better suited to serve as alternative species for mine vegetation restoration. ΔK can be used as a special marker for damage to the oxygen-evolving complex (OEC) on the donor side of PSII (Bussotti 2004). The high value of fluorescence intensity at point J indicated that the electron transfer from the primary quinone acceptor Q_A^- to the secondary quinone acceptor Q_B was inhibited, resulting in a significant accumulation of Q_A^- (Strasser and Srivastava 1995). Compared with the CK, the value of fluorescence intensity at K-step in the O–K–J–I–P curves

of *Populus* spp., *C. korshinskii*, and *A. ordosica* leaves increased significantly in SZ and CZ, indicating that the OEC of three plants in SZ and CZ was damaged under the disturbance of coal mining subsidence, and the degree of damage was higher than those in NZ and CK (Fig. 2). The value of fluorescence intensity at J step in the O–K–J–I–P curves of three plants increased significantly in SZ and CZ (Fig. 2), indicating that the photosynthetic electron transfer from Q_A^- to Q_B was inhibited, which led to the accumulation of Q_A^- and finally affected the photosynthetic efficiency of the three plant leaves in SZ and CZ.

JIP-test parameters: In this study, the JIP-test parameters of *Populus* spp., *C. korshinskii*, and *A. ordosica* leaves in SZ, CZ, NZ, and CK were compared and analyzed, including parameters, such as ABS/RC, TR₀/RC, DI₀/RC,

ET₀/RC, ET₀/TR₀, ET₀/ABS, F₀/F_m, F_v/F_m, PI_{ABS}, M₀, and DF_(abs), to provide additional evidence for the profound influence of coal mining subsidence on the structure and function of the photosynthetic apparatus of typical plant leaves. Since the parameter values described above are in different orders of magnitude, the original data require standardization to eliminate the influence of magnitude among the parameters. The data all belonged to [0, 1] after processing. The results of the standardization of JIP-test parameters of plant leaves in SZ, CZ, NZ, and CK are shown in Fig. 3 (regarding the CK).

In the JIP-test parameters, ABS/RC, TR₀/RC, DI₀/RC, and ET₀/RC, were used to indicate the energy transformation in the PSII reaction center. ET₀/TR₀, ET₀/ABS, F_v/F_m, and F₀/F_m were used to indicate the distribution of energy at the PSII acceptor side. Fig. 3 shows that, based

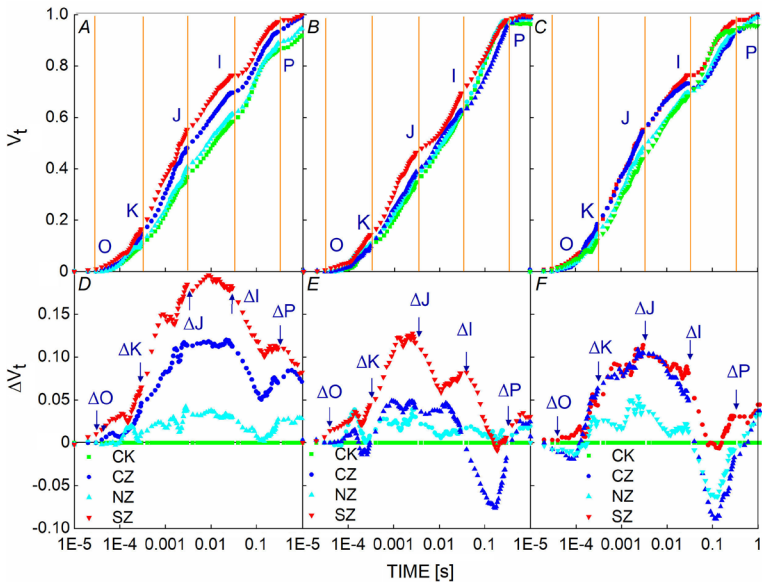


Fig. 2. The relative variable fluorescence induction kinetic curve and relative variable fluorescence difference curve of *Populus* spp. (A,D), *Caragana korshinskii* (B,E), and *Artemisia ordosica* (C,F) in CK (green line), NZ (cyan line), CZ (blue line), and SZ (red line). The means represent nine replications. CK – control area; CZ – compression zone; NZ – neutral zone; SZ – stretch zone.

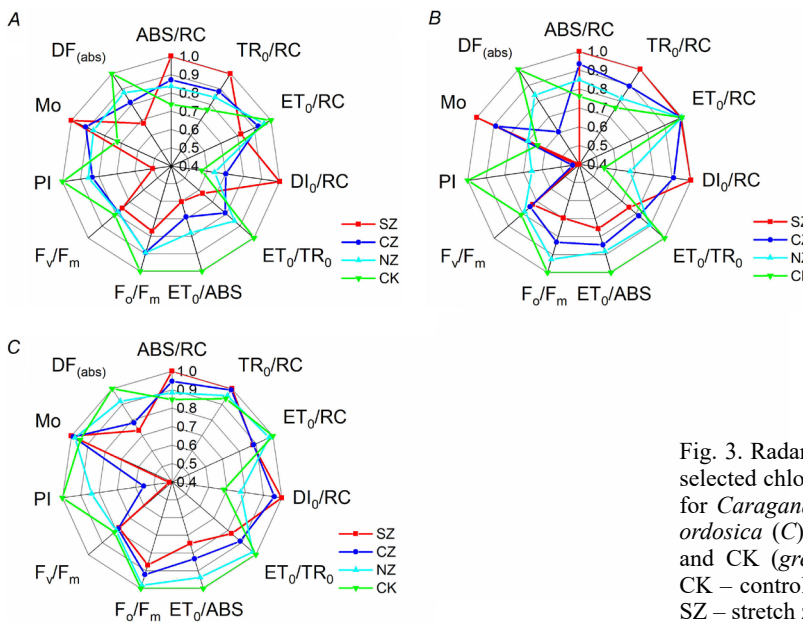


Fig. 3. Radar plots representing the changes in the values of 11 selected chlorophyll *a* fluorescence parameters from the JIP-test for *Caragana korshinskii* (A), *Populus* spp. (B), and *Artemisia ordosica* (C) in SZ (red line), CZ (blue line), NZ (cyan line), and CK (green line). The means represent nine replications. CK – control area; CZ – compression zone; NZ – neutral zone; SZ – stretch zone.

on the RC, the absorbed light energy (ABS/RC), captured light energy (TR₀/RC), and thermally dissipated light energy (DI₀/RC) on the unit of active center increased significantly under the disturbance of coal mining subsidence compared with those of the CK, while the energy used for electron transfer (ET₀/RC), the probability of electron transfer to electron acceptor downstream of Q_A⁻ in the electron transfer chain (ET₀/TR₀) and the transfer of electrons increased significantly. The quantum yield (ET₀/ABS) decreased significantly. This indicated that the electron transfer was inhibited, the light reaction activity was reduced, and the excess light energy was accumulated, which led to the decrease of the energy share of electron transfer in plant leaves. Therefore, it was necessary to reduce the stress damage caused by coal mining subsidence by increasing the dissipation by heat.

The basic principle of using the rapid Chl fluorescence induction kinetic curve to diagnose plant damage indicates that when the maximum photochemical efficiency (F_v/F_m) is less than 0.80, the plant is under stress, with declining values of F_v/F_m indicating that the degree of stress is more serious (Björkman and Demmig 1987). The results of the JIP-test parameter analysis showed that the F_v/F_m of *Populus* spp. leaves in SZ, CZ, and NZ was 0.727, 0.746, and 0.785, respectively; the F_v/F_m of *C. korshinskii* leaves was 0.753, 0.783, and 0.798, respectively, and the F_v/F_m of *A. ordosica* leaves was 0.779, 0.787, and 0.801, respectively. These results lead to the conclusion that compared to the plant species in the CK and NZ, *Populus* spp., *C. korshinskii*, and *A. ordosica* in the SZ and CZ were disturbed to a greater degree by coal mining subsidence. An analysis of the F_v/F_m value under the same degree of stress indicates that the resistance of the three plants to stress is as follows: *A. ordosica* > *C. korshinskii* > *Populus* spp. Simultaneously, it also proves that the destruction

of soil site conditions caused by coal mining subsidence indeed disturbed the growth of surface plants.

Photosynthetic parameters: Differences in photosynthetic parameters of three types of plants in different mining subsidence areas were analyzed and are shown in Fig. 4. The g_s sensitivity is an important characteristic of stress in plants (Liu *et al.* 2018). By comparing the g_s and L_s of three plants in different subsidence locations, the L_s of the three plants increased from CK to NZ and CZ and SZ in turn, while g_s decreased in turn. The stomata are the main channel for water vapor exchange between plants and the atmosphere, and they are the site at which CO₂ is absorbed from the air and the main outlet for water vapor to escape from leaves. The opening degree of stomata directly affects the P_N and E of plants (Wang *et al.* 2018b). Fig. 4 shows that the leaf E and P_N of three plants from NZ to CZ and SZ decreased in turn compared with those of the CK, and this change was closely related to the degree of opening of the leaf stomata. Part of the water absorbed by the plant roots is lost through leaf transpiration; E plays an important role in maintaining the balance of water in plants (Brito *et al.* 2018). The results showed that to maintain normal physiological activities and reduce the loss of water in plants, L_s increased and g_s decreased, which led to the decrease of E in plant leaves, also indicating that the plants in the coal mining subsidence area were likely to suffer from drought stress. The intensity of photosynthesis can be accurately reflected by Normalized Difference Vegetation Index (NDVI, Yuan *et al.* 2016). The decrease of g_s in plants in the coal mining subsidence area not only reduced the water loss of leaves but also reduced the absorption of CO₂ from the air. As one of the essential sources for reactions in plant photosynthesis, the long-term reduction

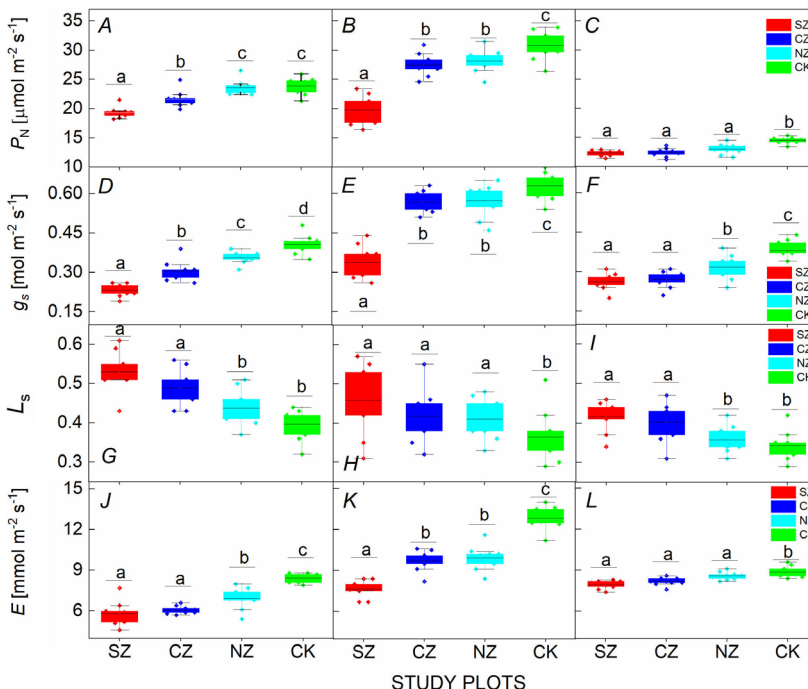


Fig. 4. Comparison of photosynthetic parameters of *Populus* spp. (A,D,G,J), *Caragana korshinskii* (B,E,H,K), and *Artemisia ordosica* (C,F,I,L) leaves in SZ (red), CZ (blue), NZ (cyan), and CK (green), respectively. Different underlined lowercase letters indicate a significant difference between four different study plots ($p<0.05$). The means represent nine replications. E – transpiration rate; g_s – stomatal conductance; L_s – stomatal limitation; P_N – photosynthetic CO₂ assimilation rate. CK – control area; CZ – compression zone; NZ – neutral zone; SZ – stretch zone.

of the concentration of CO_2 would directly affect the P_N of plant leaves, and then affect the biomass and NDVI in coal mining subsidence areas.

Correlation analysis: The relationship between soil physico-chemical properties (SWC, OM, TN, TP, AN, NN, and BD), JIP-test parameters (F_v/F_m , F_v/F_0 , PI_{ABS} , M_0 , ABS/RC , ET_0/RC , DI_0/RC , ET_0/TR_0 , DF_{abs} , and TR_0/RC) and photosynthetic gas-exchange indices (P_N , L_s , g_s , and E) are shown in Fig. 5. The SWC significantly negatively correlated with ABS/RC , TR_0/RC , and DI_0/RC , with correlation coefficients of -0.789 , -0.902 , and -0.786 , respectively. A significant positive correlation was observed among the SWC and PI_{ABS} , F_0/F_m , F_v/F_m , g_s , ET_0/ABS , ET_0/TR_0 , E , and P_N with correlation coefficients of 0.636 , 0.704 , 0.754 , 0.778 , 0.717 , 0.798 , 0.601 , and 0.746 , respectively. Also, other soil physico-chemical factors correlated with the photosynthetic parameters of individual plants to some degree. For example, the OM positively correlated with the M_0 and ABS/RC , with correlation coefficients of 0.607 and 0.70 , respectively. The TN negatively correlated with ET_0/TR_0 , with correlation coefficient of -0.468 . The TP negatively correlated with PI_{ABS} and ET_0/TR_0 , with correlation coefficients of -0.509 and -0.296 , respectively. However, in general, these soil factors only correlated with one or a few photosynthesis

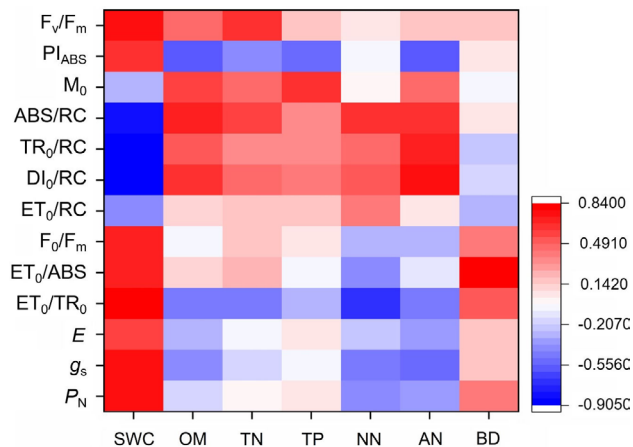


Fig. 5. Correlation between JIP-test parameters, photosynthesis indexes, and soil physico-chemical properties. *Red* means positive correlation, *blue* means negative correlation, the deeper the color, the higher the correlation.

indices, and the correlation coefficients were low. These low degrees of correlation indicate that the SWC is one of the key soil physico-chemical factors that affect plant JIP-test parameters and photosynthesis indices in semiarid mining subsidence areas. The results are consistent with many studies on the relationship between vegetation growth and soil environmental factors in coal mining areas in the Loess Plateau (Lei *et al.* 2016, Wang *et al.* 2017, Yang *et al.* 2018b, Liu *et al.* 2019c).

Analysis of the transfer process of coal mining subsidence to individual plant damage

Strata breaking and movement to soil subsidence and deformation above the goaf: Underground coal mining forms a large area of goaf, which destroys the equilibrium state of rock stress, causes the redistribution of stress in rock masses, and leads to rock fracture and movement. The redistribution of the blocks formed after the breakage and movement of hard rock strata inevitably changes the initial state of the overlying strata in the goaf. The overlying movement of the strata eventually forms the mining overburden movement profile dominated by the key layers as shown in Fig. 6. Typically, curved subsidence, fracture, and collapse zones are formed above the goaf. When the movement of rock strata tends to be stable again after the breakage of the key strata, the fissures of rock strata are closed again, forming a recompaction area; for the violent movement of rock strata, the areas with drastic changes in ground pressure, fractures and collapse are called fracture development areas.

From soil subsidence deformation to plant growth site condition changes: With the process of soil subsidence and deformation in the goaf, the conditions for plant habitats on the surface have changed, which primarily manifests in changes in topography (Blachowski and Milczarek 2014), groundwater depth (Lei and Bian 2014), surface SWC (Liu and Li 2019), and soil physical and chemical properties (Feng *et al.* 2019). On the one hand, the impact of underground coal mining usually results in the pumping and draining of groundwater to prevent water inrush accidents in the working face during the preparation stage before mining (Ma *et al.* 2019), which inevitably reduces the groundwater level of working face and affects the recharge of groundwater to the SWC. When the depth of groundwater level increases, the recharge of surface soil by capillary water

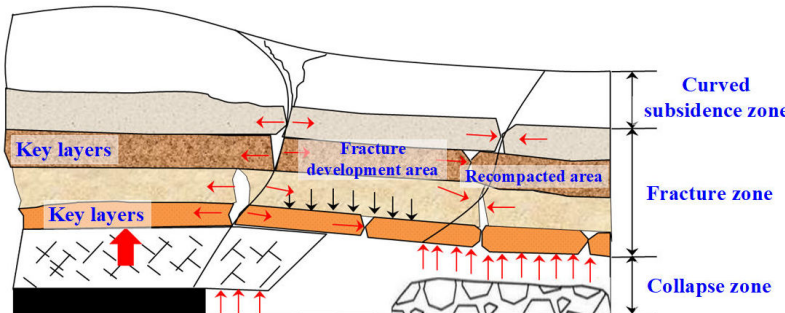


Fig. 6. Movement division of overlying strata in the goaf of underground mining.

decreases, and the soil water rapidly evaporates, leading to the decrease in SWC. When the SWC cannot meet the needs of plant physiological activities, it causes drought stress on plant growth (Lei 2010). Therefore, the ground-water depth also has an important impact on the SWC, which is another key determinant to control the growth of surface vegetation in semiarid mining areas.

The influence of underground coal mining on the SWC results in spatial heterogeneity in different subsidence locations. The NZ is located in the center of surface subsidence basin. Along the mining face, the terrain tends to be high on both sides and low in the middle. This terrain is conducive to the collection of surface runoff, resulting in higher SWC in the NZ than that in the CZ and SZ. The soil in the CZ is compressed, and the porosity, hardness and capacity of the soil for infiltration are reduced, which is not conducive to the conservation of soil water. Therefore, compared with the NZ, the SWC in CZ is generally lower. There are permanent cracks on the surface of the SZ, which changes the direction of surface runoff and catchment conditions to some extent. When the surface cracks are directly connected with the goaf, the surface runoff will flow directly into the goaf. In addition, permanent cracks will lead to the increase in the surface area of the evaporation of soil water, which also increases the speed of the evaporation of soil water and its dissipation.

From disturbance of growth site conditions to photosynthesis changes in plant leaves: The photosynthetic gas exchange of plant leaves changes in parallel with the growth site conditions of the plants. The deformation

process and final form of existence of the soil in SZ, CZ, and NZ areas differ. After mining subsidence, the habitat conditions above show some spatial heterogeneity in these 'three areas', and the response of plant growth to habitat change also differs spatially. The SWC is undoubtedly the most important limiting factor for plant growth in the semiarid mining area of the Loess Plateau (Liu *et al.* 2018). Wang *et al.* (2010) studied the water source of plants in the Shendong mining area using the principle of stable isotope fractionation. The results showed that the water needed for plant growth in this area primarily originates from soil water. The photosynthetic parameters of plants respond to the changes in SWC. In this study, the Chl fluorescence and photosynthetic gas-exchange parameters of *A. ordosica*, *C. korshinskii*, and *Populus* spp. leaves in the 'three areas' and CK were comprehensively compared and analyzed. The L_s of the three plants increased in turn from the NZ to the SZ, and g_s , P_N , and E were lower in turn. The fast Chl fluorescence induction curve changed from O-J-I-P to O-K-J-I-P. The analysis of the JIP-test parameters under the influence of coal mining subsidence indicated that the share of energy of plant leaves for electron transfer was reduced, and the transfer of electrons was gradually inhibited. Thus, the photosynthetic efficiency of plant leaves decreased. Wang *et al.* (2014) found that the K-step appeared in the Chl fluorescence induction kinetics curves of plants under drought stress. The changes in the photosynthetic gas-exchange parameters in this study are consistent with the changes of SWC in the 'three areas'. The results showed that the disturbance of coal mining subsidence led to a decrease in SWC, and the three plants were subjected

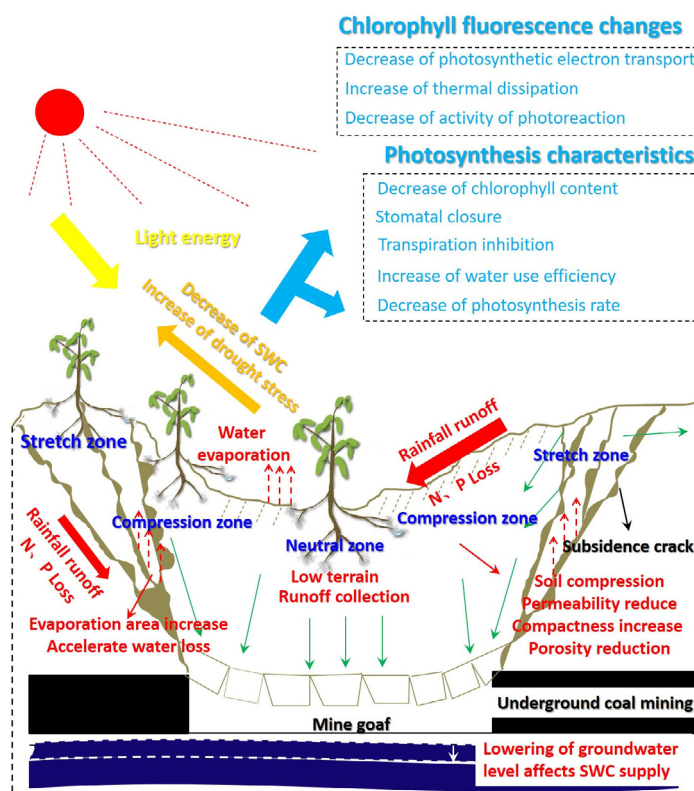


Fig. 7. Schematic diagram of the transmission process of influence of coal mining subsidence on plant growth in semiarid region.

to different degrees of drought stress. The degree of plant drought stress in the SZ was higher than that in the CZ while it was the lowest in the NZ.

The transfer process of disturbance of coal mining subsidence on plant growth in a semiarid area is summarized in Fig. 7.

Conclusions: In this study, the response of the disturbance of surface plants in underground coal mining was diagnosed and analyzed at an individual scale. The micro-ecological mechanism implied in the macro-response of vegetation disturbance in underground coal mining was revealed using O-J-I-P chlorophyll *a* fluorescence analysis. The rapid chlorophyll fluorescence induction curve of different plant leaves was deformed when the plants were disturbed by coal mining subsidence; the L_s of leaves increased; g_s , P_N , and E decreased significantly, and the plant leaves reduced their share of energy for electron transfer, which also led to the inhibition of photosynthetic electron transfer and the decrease in photosynthetic efficiency of the plants. Correlation analysis indicated that the SWC was the key soil physico-chemical factor that affects the physiological characteristics of the photosynthesis of plant leaves in a subsidence area. The analysis of three important processes of the influence of mining subsidence disturbance on the physiological characteristics of the photosynthesis of individual plants led to the conclusion that the deformation process and the final existence of the form of soil in the stretch, compression, and neutral zones differ, which leads to the spatial heterogeneity of the SWC after mining subsidence. This is the reason for the spatial difference of the photosynthetic physiological response of plants in different subsidence areas. These results provide a methodological basis for the restoration of vegetation in disturbed areas for this mining area and similar areas.

References

Bian Z., Lei S., Jin D. *et al.*: [Several basic scientific issues related to mined land remediation.] – *J. China Coal Soc.* **43**: 190-197, 2018. [In Chinese] doi: 10.13225/j.cnki.jccs.2017.4004.

Björkman O., Demmig B.: Photon yield of O_2 evolution and chlorophyll fluorescence characteristics at 77 K among vascular plants of diverse origins. – *Planta* **170**: 489-504, 1987.

Blachowski J., Milczarek W.: Analysis of surface changes in the Wałbrzych hard coal mining grounds (SW Poland) between 1886 and 2009. – *Geol. Q.* **58**: 353-368, 2014.

Brestic M., Zivcak M., Kalaji H.M. *et al.*: Photosystem II thermostability *in situ*: Environmentally induced acclimation and genotype-specific reactions in *Triticum aestivum* L. – *Plant Physiol. Bioch.* **57**: 93-105, 2012.

Brito C., Dinis L.-T., Ferreira H. *et al.*: The role of nighttime water balance on *Olea europaea* plants subjected to contrasting water regimes. – *J. Plant Physiol.* **226**: 56-63, 2018.

Bussotti F.: Assessment of stress conditions in *Quercus ilex* L. leaves by O-J-I-P chlorophyll *a* fluorescence analysis. – *Plant Biosyst.* **138**: 101-109, 2004.

Carstensen A., Szameitat A.E., Frydenvang J., Husted S.: Chlorophyll *a* fluorescence analysis can detect phosphorus deficiency under field conditions and is an effective tool to prevent grain yield reductions in spring barley (*Hordeum vulgare* L.). – *Plant Soil* **434**: 79-91, 2019.

Chen X., Wong J.T., Leung A.O. *et al.*: Comparison of plant and bacterial communities between a subtropical landfill topsoil 15 years after restoration and a natural area. – *Waste Manag.* **63**: 49-57, 2017.

Chiochetta C.G., Toumi H., Böhm R.F.S. *et al.*: Use of phytoproductivity data in the choice of native plant species to restore a degraded coal mining site amended with a stabilized industrial organic sludge. – *Environ. Sci. Pollut. R.* **24**: 24624-24633, 2017.

Clifford M.J., Ali S.H., Matsubae K.: Mining, land restoration and sustainable development in isolated islands: An industrial ecology perspective on extractive transitions on Nauru. – *Ambio* **48**: 397-408, 2019.

Dąbrowski P., Baczewska A.H., Pawluśkiewicz B. *et al.*: Prompt chlorophyll *a* fluorescence as a rapid tool for diagnostic changes in PSII structure inhibited by salt stress in Perennial ryegrass. – *J. Photoch. Photobio. B* **157**: 22-31, 2016.

Dąbrowski P., Pawluśkiewicz B., Baczewska-Dąbrowska A.H. *et al.*: Chlorophyll *a* fluorescence of perennial ryegrass (*Lolium perenne* L.) varieties under long term exposure to shade. – *Zemdirbyste* **102**: 305-312, 2015.

Darmody R.G., Bauer R., Barkley D. *et al.*: Agricultural impacts of longwall mine subsidence: the experience in Illinois, USA and Queensland, Australia. – *Int. J. Coal Sci. Technol.* **1**: 207-212, 2014.

Eckert S., Hüsler F., Liniger H., Hodel E.: Trend analysis of MODIS NDVI time series for detecting land degradation and regeneration in Mongolia – *J. Arid Environ.* **113**: 16-28, 2015.

Feng Y., Wang J., Bai Z., Reading L.: Effects of surface coal mining and land reclamation on soil properties: A review. – *Earth-Sci. Rev.* **191**: 12-25, 2019.

Gray D.W., Cardon Z.G., Lewis L.A.: Simultaneous collection of rapid chlorophyll fluorescence induction kinetics, fluorescence quenching parameters, and environmental data using an automated PAM-2000/CR10X data logging system. – *Photosynth. Res.* **87**: 295-301, 2006.

He G.: [Mining Subsidence Science.] Pp. 57-74. China University of Mining and Technology Press, Xuzhou 1991. [In Chinese]

Hu Z., Xiao W., Zhao Y.: [Re-discussion on coal mine eco-environment concurrent mining and reclamation.] – *J. China Coal Soc.* **45**: 351-359, 2020. [In Chinese] doi: 10.13225/j.cnki.jccs.YG19.1694.

Jia Z.: [Temporal and spatial characteristics and driving forces of vegetation coverage in typical mining areas in Shanxi Province.] Pp. 10-78. Shanxi Agricultural University, Jinzhong 2018. [In Chinese]

Kalaji H.M., Račková L., Paganová V. *et al.*: Can chlorophyll-*a* fluorescence parameters be used as bioindicators to distinguish between drought and salinity stress in *Tilia cordata* Mill? – *Environ. Exp. Bot.* **152**: 149-157, 2018.

Karan S.K., Samadder S.R.: A comparison of different land-use classification techniques for accurate monitoring of degraded coal-mining areas. – *Environ. Earth Sci.* **77**: 713, 2018.

Lechner A.M., Baumgartl T., Matthew P., Glenn V.: The impact of underground longwall mining on prime agricultural land: a review and research agenda. – *Land Degrad. Dev.* **27**: 1650-1663, 2016.

Lei S.: [Monitoring and analyzing the mining impacts on key environmental elements in desert area.] – *J. China Coal Soc.* **35**: 1587-1588, 2010. [In Chinese] doi: 10.13225/j.cnki.jccs.2010.09.028.

Lei S., Bian Z.: [Research progress on the environment impacts from underground coal mining in arid western area of China.] – *Acta Ecol. Sin.* **34**: 2837-2843, 2014. [In Chinese] doi: 10.5846/stxb201307281968.

Lei S., Ren L., Bian Z.: Time–space characterization of vegetation in a semiarid mining area using empirical orthogonal function decomposition of MODIS NDVI time series. – *Environ. Earth Sci.* **75**: 516, 2016.

Li X., Lei S., Cheng W. *et al.*: Spatio-temporal dynamics of vegetation in Jungar Banner of China during 2000–2017. – *J. Arid Land* **11**: 837-854, 2019.

Liu S., Li W.: Zoning and management of phreatic water resource conservation impacted by underground coal mining: A case study in arid and semiarid areas. – *J. Clean. Prod.* **224**: 677-685, 2019.

Liu S., Li W., Qiao W. *et al.*: Effect of natural conditions and mining activities on vegetation variations in arid and semiarid mining regions. – *Ecol. Indic.* **103**: 331-345, 2019c.

Liu Y., Lei S., Cheng L. *et al.*: [Effects of soil water content on stomatal conductance, transpiration, and photosynthetic rate of *Caragana korshinskii* under the influence of coal mining subsidence.] – *Acta Ecol. Sin.* **38**: 3069-3077, 2018. [In Chinese] doi: 10.5846/stxb201703160442.

Liu Y., Lei S., Cheng L. *et al.*: Leaf photosynthesis of three typical plant species affected by the subsidence cracks of coal mining: a case study in the semiarid region of Western China. – *Photosynthetica* **57**: 75-85, 2019a.

Liu Y., Lei S., Gong C.: Comparison of plant and microbial communities between an artificial restoration and a natural restoration topsoil in coal mining subsidence area. – *Environ. Earth Sci.* **78**: 204, 2019b.

Luo Y.: [Systematic approach to assess and mitigate longwall subsidence influences on surface structures.] – *J. Coal Sci. Eng.* **14**: 407-414, 2008. [In Chinese] doi: 10.1007/s12404-008-0090-5.

Lv W.Y.: The mitigation of surface subsidence in coal mines. – *Energ. Environ.* **27**: 350-359, 2016.

Ma K., Zhang Y., Ruan M. *et al.*: Land subsidence in a coal mining area reduced soil fertility and led to soil degradation in arid and semi-arid regions. – *Int. J. Environ. Res. Public Health* **16**: 3929, 2019.

Ma L., Zhao B., Xu H. *et al.*: [Research on water inrush mechanism of fault coupling bed separation with fully mechanized sublevel caving of ultra thick coal seam.] – *J. China Coal Soc.* **44**: 567-575, 2019. [In Chinese] doi: 10.13225/j.cnki.jccs.2018.0593.

Mehta P., Jajoo A., Mathur S., Bharti S.: Chlorophyll *a* fluorescence study revealing effects of high salt stress on Photosystem II in wheat leaves. – *Plant Physiol. Bioch.* **48**: 16-20, 2010.

Rošer J., Potočnik D., Vulić M.: Analysis of dynamic surface subsidence at the underground coal mining site in Velenje, Slovenia through modified sigmoidal function. – *Minerals* **8**: 74, 2018.

Singh S., Prasad S.M.: IAA alleviates Cd toxicity on growth, photosynthesis and oxidative damages in eggplant seedlings. – *Plant Growth Regul.* **77**: 87-98, 2015.

Strasser R.J., Srivastava A.: Polyphasic chlorophyll *a* fluorescence transient in plants and cyanobacteria. – *Photochem. Photobiol.* **61**: 32-42, 1995.

Strasser R.J., Tsimilli-Michael M., Srivastava A.: Analysis of the chlorophyll *a* fluorescence transient. – In: Papageorgiou G.C., Govindjee (ed.): *Chlorophyll *a* Fluorescence: A Signature of Photosynthesis. Advances in Photosynthesis and Respiration.* Pp. 321-362. Springer, Dordrecht 2004.

Su X., Wang M., Shu S. *et al.*: [Effects of exogenous Spd on the fast chlorophyll fluorescence induction dynamics in tomato seedlings under high temperature stress.] – *Acta Hortic. Sin.* **40**: 2409-2418, 2013. doi: 10.16420/j.issn.0513-353x.2013.12.011. [In Chinese]

Sun S., Sun H., Zhang D. *et al.*: Response of soil microbes to vegetation restoration in coal mining subsidence areas at Huabei coal mine, China. – *Int. J. Environ. Res. Public Health* **16**: 1757, 2019.

Vereecken H., Pachepsky Y., Simmer C. *et al.*: On the role of patterns in understanding the functioning of soil-vegetation-atmosphere systems. – *J. Hydrol.* **542**: 63-86, 2016.

Wang J., Kang H., Liu J. *et al.*: [Layout strategic research of green coal resources development in China.] – *J. China Univ. Min. Technol.* **47**: 15-20, 2018a. [In Chinese] doi: 10.13247/j.cnki.jcumt.000793.

Wang J., Wang P., Qin Q., Wang H.: The effects of land subsidence and rehabilitation on soil hydraulic properties in a mining area in the Loess Plateau of China. – *Catena* **159**: 51-59, 2017.

Wang L., Wei S., Zhang Q. *et al.*: [Isotopic characteristics of water within the soil-vegetation atmosphere system in the Yushenfu mining area.] – *J. China Coal Soc.* **35**: 1347-1353, 2010. [In Chinese] doi: 10.13225/j.cnki.jccs.2010.08.001.

Wang Q., Zhao M.: [Effects of coal resources exploitation on the water resource and vegetation in arid and semi-arid region.] – *J. Water Res. Water Eng.* **28**: 77-81, 2017. [In Chinese] doi: 10.11705/j.issn.1672-643X.2017.03.15.

Wang X., Du T., Huang J. *et al.*: Leaf hydraulic vulnerability triggers the decline in stomatal and mesophyll conductance during drought in rice. – *J. Exp. Bot.* **69**: 4033-4045, 2018b.

Wang X., Li Y., Wei Y. *et al.*: Effects of fertilization and reclamation time on soil bacterial communities in coal mining subsidence areas. – *Sci. Total Environ.* **739**: 139882, 2020.

Wang Z., Chen L., Ai J. *et al.*: [Effects of different drought stress on photosynthesis and activity of photosystem II in leaves of Amur grape (*Vitis amurensis*).] – *Plant Physiol. J.* **50**: 1171-1176, 2014. [In Chinese] doi: 10.13592/j.cnki.ppj.2014.08.001.

Yang D.J., Bian Z.F., Lei S.G.: Impact on soil physical qualities by the subsidence of coal mining: a case study in Western China. – *Environ. Earth Sci.* **75**: 652, 2016.

Yang X., Sun X., Huang J. *et al.*: [Analysis of driving factors and prevention measures for desertification in Muli coal mining area in Qinghai Province.] – *Chin. J. Geol. Hazard Control* **29**: 78-84, 2018b. [In Chinese] doi: 10.16031/j.cnki.issn.1003-8035.2018.01.13.

Yang Y., Erskine P.D., Zhang S. *et al.*: Effects of underground mining on vegetation and environmental patterns in a semiarid watershed with implications for resilience management. – *Environ. Earth Sci.* **77**: 605, 2018a.

Yu M., Gao Q., Gao S.: An ecophysiological model for individual plant under global change. – *Acta Bot. Sin.* **39**: 811-820, 1997.

Yuan L., Zhang N., Kan J. *et al.*: [The concept, model and reserve forecast of green coal resources in China.] – *J. China Univ. Min. Technol.* **47**: 1-8, 2018. [In Chinese] doi: 10.13247/j.cnki.jcumt.000792.

Yuan X., Zou L., Lin A. *et al.*: [Analyzing dynamic vegetation change and response to climatic factors in Hubei Province, China.] – *Acta Ecol. Sin.* **36**: 5315-5323, 2016. [In Chinese] doi: 10.5846/stxb201507101464.

Zhang Z., Wang C., Tang Y. *et al.*: Analysis of ground subsidence at a coal-mining area in Huainan using time-series InSAR. – *Int. J. Remote Sens.* **36**: 5790-5810, 2015.

Zushii K., Matsuzoe N.: Using of chlorophyll *a* fluorescence OJIP transients for sensing salt stress in the leaves and fruits of tomato. – *Sci. Hortic.-Amsterdam* **219**: 216-221, 2017.